







Article

The Effect of Chopped Carbon Fibers on the Mechanical Properties and Fracture Toughness of 3D-Printed PLA Parts: An Experimental and Simulation Study

Ahmed Ali Farhan Ogaili ¹ , Ali Basem ², Mohammed Salman Kadhim ³, Zainab T. Al-Sharif ^{4,5} , Alaa Abdulhady Jaber ^{6,*} , Emad Kadum Njim ⁷ , Luttfi A. Al-Haddad ⁸ , Mohsin Noori Hamzah ⁶  and Ehsan S. Al-Ameen ¹

- ¹ Mechanical Engineering Department, College of Engineering, Mustansiriyah University, Baghdad 10052, Iraq; ahmed_ogaili@uomustansiriyah.edu.iq (A.A.F.O.); apehsanameen@uomustansiriyah.edu.iq (E.S.A.-A.)
- ² Air Conditioning Engineering Department, Faculty of Engineering, Warith Al-Anbiyaa University, Karbala 56001, Iraq; ali.basem@uowa.edu.iq
- ³ Applied Science Department, University of Technology, Baghdad 10066, Iraq; 100358@uotechnology.edu.iq
- ⁴ Environmental Engineering Department, Al Hikma University College, Baghdad 10052, Iraq; zta011@alumni.bham.ac.uk
- ⁵ Chemical Engineering Department, Birmingham University, Birmingham B15 2TT, UK
- ⁶ Mechanical Engineering Department, University of Technology-Iraq, Baghdad 10066, Iraq; mohsin.n.hamzah@uotechnology.edu.iq
- ⁷ Ministry of Industry and Minerals, State Company for Rubber and Tires Industries, Baghdad 10052, Iraq; emad.njim@gmail.com
- ⁸ Training and Workshops Center, University of Technology-Iraq, Baghdad 19006, Iraq; luttfi.a.alhaddad@uotechnology.edu.iq
- * Correspondence: alaa.a.jaber@uotechnology.edu.iq



Citation: Ogaili, A.A.F.; Basem, A.; Kadhim, M.S.; Al-Sharif, Z.T.; Jaber, A.A.; Njim, E.K.; Al-Haddad, L.A.; Hamzah, M.N.; Al-Ameen, E.S. The Effect of Chopped Carbon Fibers on the Mechanical Properties and Fracture Toughness of 3D-Printed PLA Parts: An Experimental and Simulation Study. *J. Compos. Sci.* **2024**, *8*, 273. <https://doi.org/10.3390/jcs8070273>

Academic Editor: Yuan Chen

Received: 20 June 2024

Revised: 9 July 2024

Accepted: 12 July 2024

Published: 15 July 2024



Copyright: © 2024 by the authors. Licensee MDPI, Basel, Switzerland. This article is an open access article distributed under the terms and conditions of the Creative Commons Attribution (CC BY) license (<https://creativecommons.org/licenses/by/4.0/>).

Abstract: The incorporation of fiber reinforcements into polymer matrices has emerged as an effective strategy to enhance the mechanical properties of composites. This study investigated the tensile and fracture behavior of 3D-printed polylactic acid (PLA) composites reinforced with chopped carbon fibers (CCFs) through experimental characterization and finite element analysis (FEA). Composite samples with varying CCF orientations (0° , $0^\circ/90^\circ$, $+45^\circ/-45^\circ$, and $0^\circ/+45^\circ/-45^\circ/90^\circ$) were fabricated via fused filament fabrication (FFF) and subjected to tensile and single-edge notched bend (SENB) tests. The experimental results revealed a significant improvement in tensile strength, elastic modulus, and fracture toughness compared to unreinforced PLA. The $0^\circ/+45^\circ/90^\circ$ orientation exhibited a 3.6% increase in tensile strength, while the $+45^\circ/-45^\circ$ orientation displayed a 29.9% enhancement in elastic modulus and a 29.9% improvement in fracture toughness (259.12 MPa) relative to neat PLA (199.34 MPa \sqrt{m}). An inverse correlation between tensile strength and fracture toughness was observed, attributed to mechanisms such as crack deflection, fiber bridging, and fiber pull-out facilitated by multi-directional fiber orientations. FEA simulations incorporating a transversely isotropic material model and the J-integral approach were conducted using Abaqus, accurately predicting fracture toughness trends with a maximum discrepancy of 8% compared to experimental data. Fractographic analysis elucidated the strengthening mechanisms, highlighting the potential of tailoring CCF orientation to optimize mechanical performance for structural applications.

Keywords: AM; 3D printing; PLA/CF; experimental tests; FEM

1. Introduction

Additive manufacturing (AM), more commonly referred to as three-dimensional (3D) printing, is a disruptive technology that allows the manufacture of complex geometries with a level of precision and accuracy that has potential to be improved [1,2]. Additive manufacturing (AM) has revolutionized the production of complex geometries with unprecedented

precision and accuracy [3,4]. One of the key advantages of 3D printing, especially fused filament fabrication (FFF), is its ability to significantly enhance mechanical properties through the incorporation of reinforcing materials [5,6]. Among the many materials applied in additive manufacturing, polylactic acid (PLA) is well liked, not only for its biodegradability and renewability, but also because it is biocompatible [7,8]. PLA is a kind of thermoplastic polyester; it is derived from renewable sources such as corn starch or sugarcane and is an environmentally friendly type of plastic [5]. However, this resin often has relatively inferior mechanical properties, such as brittleness and poor impact strength, which results in limitations to its applications in many areas where high mechanical performance is needed.

Compared to traditional manufacturing methods, which often involve subtractive processes leading to material wastage, 3D printing is highly efficient and environmentally friendly. The integration of carbon fibers into PLA (polylactic acid) matrices has been particularly noteworthy. Carbon fibers enhance the mechanical properties of PLA by providing superior tensile strength, fracture toughness, and durability. This is attributed to carbon fibers' high strength-to-weight ratio, excellent stiffness, and thermal stability, making the resulting PLA–carbon fiber composites suitable for high-performance engineering applications. These enhancements are crucial for expanding the applicability of PLA in load-bearing and structural components—applications where pure PLA would traditionally fall short due to its inherent mechanical limitations.

Among the various AM techniques, fused filament fabrication (FFF) or fused deposition modeling (FDM)—a popular technique—has the advantages of easy use, low cost, and processing of a wide range of thermoplastic materials [5,6]. Additive manufacturing (AM) has now been termed the new era of manufacturing, mainly because it allows increasing complexity in the production of substances across a diverse range of industries, such as aerospace, automobile, biomedical, and consumer products [7,9,10]. The utilization of FDM has been pursued in AM strategies because of its cost-effectiveness, ease of use, and flexibility [11,12]. MAKINGPLA is advantageous; however, its applicability in load-bearing and structural components has been restricted by its intrinsic mechanical deficiencies, such as low strength, stiffness, and fracture toughness [13].

Recent advancements in 3D printing have facilitated the exploration of various composite materials to enhance mechanical properties. Significant research has been carried out to enhance the mechanical performance of PLA by the addition of reinforcing materials, in particular, carbon fibers (CFs). The addition of reinforcing materials, especially carbon fibers, has been used to enhancing PLA's mechanical properties and fracture toughness for components designed for 3D printing. Numerous research studies have been conducted on the effect of both chopped and continuous carbon fibers on the properties of PLA matrices. Knowledge of the effects of chopped carbon fibers on the properties of 3D-PLA parts can be used to develop new advanced composites for application as AM products with tailor-made properties [14].

One study addressed the circular economy by converting waste polypropylene (PP) and carbon fibers into upcycled composite materials suitable for additive manufacturing. This research optimized material extrusion and 3D printing to overcome adhesion and warpage issues, examining the effects of various carbon fiber weight fractions on filament properties and printability. The results highlighted the successful fabrication of fiber-reinforced filaments despite some reduction in mechanical properties due to thermal processes during production [15]. Another study explored the micromechanics of short carbon fiber-reinforced thermoplastics (sCFRTP) produced via 3D printing. This investigation analyzed the effects of different printing parameters on tensile properties and internal structure through tensile testing, X-ray computed tomography, and theoretical analysis. The study found that fiber length, void volume, and fiber orientation significantly impacted mechanical properties, with optimal parameters enhancing Young's moduli and tensile strengths [16]. Additionally, research on 3D-printed continuous fiber-reinforced PA6 composites examined their degradation in salt water. Using a Markforged® Mark Two 3D printer, the study fabricated samples reinforced with carbon, glass, and Kevlar fibers. Me-

chanical tests post-ageing in saltwater revealed significant reductions in tensile and flexural strengths, with carbon fiber-reinforced samples showing the least degradation [17]. One of the most promising routes towards the enhancement of the strength, stiffness, and fracture toughness of PLA-based composites is reinforcing them with chopped carbon fibers. As a result, there is a need for further research to assess the impact of chopped carbon fiber reinforcement on both the mechanical properties and the fracture toughness of 3D-printed PLA parts [11,12]. Much research effort has already been devoted to developing strategies for improving the mechanical performance of PLA, such as the addition of different reinforcing fillers. Vălean et al. [18] conducted static and fatigue trials of 3D-printed PLA and PLA short carbon fiber-reinforced parts. They found that the addition of short carbon fibers resulted in a significant improvement in the tensile strength, fracture toughness, and fatigue life of the specimens. Iragi et al. [19] researched the ply and interlaminar behaviors of 3D-printed continuous carbon fiber-reinforced thermoplastic laminates, relating these to processing conditions and microstructure. Their study revealed the importance of process parameter optimization and showed good potential regarding the targeted mechanical properties.

Li et al. [20] studied a binding layer of a carbon fiber/PLA in FDM samples, and tensile strength and elastic modulus improvements were recorded. Another study [21] designed and cohesively tested structurally alternate-layered polymer composites using PLA material and carbon fiber-reinforced PLA. The studies showed the intended applications of the composites and the good prospects of using them as carbon fiber-reinforced materials. It has been reported that the lower melt flow rate (MFR) of PLA/CCF samples enhanced interfilament adhesion, which significantly improved the mechanical properties of the composite [22]. The strong adhesion forces between the filaments lead to enhanced mechanical performance. Additionally, the homogeneous orientation of the CCFs within the PLA/CCF matrix facilitates effective load transfer and absorption from external forces, thereby further enhancing the mechanical properties [23]. Moreover, the uniformly dispersed carbon fibers act as heterogeneous nucleation sites, reducing the crystallization temperature of PLA and increasing its degree of crystallinity. These changes in crystallization behavior resulted in improved mechanical properties of PLA/CCF composites compared to pure PLA samples [24]. In addition to short carbon fibers, continuous carbon fibers have been considered for use with PLA matrices in additive manufacturing applications. Wang et al. [25] studied the preparation of continuous carbon fiber-reinforced PLA prepreg filaments, while Li et al. [26] studied the mechanical performances of continuous carbon fiber-reinforced PLA composites printed in vacuum environments.

Naranjo-Lozada et al. [27] compared the tensile properties and failure behavior of chopped and continuous carbon fiber composites manufactured by additive manufacturing. Their study showed the better mechanical performance of the continuous fiber composites in comparison to their chopped counterparts. Yadav et al. [28] studied the flexural strength and surface profiling of carbon-based PLA parts developed by additive manufacturing. The results showed that carbon fiber reinforcement has the potential for achieving improved flexural performance of 3D-printed PLA components. However, further research will be required in order to fully optimize processing conditions, fiber content, and material compositions with the intention of fully exploiting the advantages of reinforced composites for a wide range of applications in additive manufacturing. Few researchers have published their work due to the influence of several factors on the mechanical properties of PLA in 3D printing. The present study gives an account of the conspicuous factors that have been identified for altering the mechanical properties of PLA in 3D printing. Similarly, Kumar Patro et al. [29] worked on the mechanical properties of 3D-printed sandwich structures developed using PLA and acrylonitrile butadiene styrene (ABS). The conclusion derived from this study was that the infill pattern, layer thickness, and raster angle had a significant effect on the mechanical properties of the sandwich structures developed using this infill. The samples developed with a hexagonal infill pattern and a 0° raster angle had the highest tensile strengths and tensile moduli. Zwawi [30] evaluated the integrity of a structure and PLA 3D-printed eye grab hooks' fracture prediction with different cross-sections, and it

was concluded that the mechanical behavior of the hooks was significantly influenced by the cross-sectional shape and size. More specifically, hooks with a rectangular cross-section showed better strength together with fracture toughness compared to those featuring a circular cross-section. Wu et al. [31] studied the influence of layer thickness, raster angle, deformation temperature, and recovery temperature of shape memory on 3D-printed PLA samples. The study found that it was mainly the angle of the raster and the deformation temperature that influenced the shape memory effect. It was shown that samples achieved the most significant shape memory effect at a deformation temperature of 60 °C with a change in raster angle of 0°. Kartikeyan et al. [5] found that the mechanical properties of specimens fabricated by FDM 3D printing were affected by the relation between layer thickness, raster angle, and build orientation. The tensile strength and modulus results indicated that the best performance was achieved by a specimen with a 0° raster angle and a build orientation in parallel with the loading direction. Sajjadi et al. [32] also presented a study on 3D-printed high-impact polystyrene fracture properties with and without raster angles based on essential work of the fracture method.

Each research work showed that the raster angle exerts a remarkable influence on the fracture toughness of HIPS specimens, whereas specimens with a 0° raster angle exhibit higher fracture toughness. Ayatollahi et al. [33] studied the in-plane raster angle effect on the tensile and fracture strengths of 3D-printed PLA specimens. Therefore, the raster angle dominated the mechanical behavior of the specimens. It has been indicated that the tensile and fracture strengths are higher for specimens with a 0° raster angle. Another experimental investigation [34] evaluated a 3D-printed ABS specimen under tension–tear loading and the influence of raster orientation on fracture behavior. The results showed that raster orientation noticeably contributed to the fracture toughness and flexibility of the specimen. Therefore, the specimen with a raster angle of 90° showed larger values of fracture toughness and ductility. Gongabadi et al. [35] studied the influence of raster angle, build orientation, and infill density on the elasticity of 3D-printed parts. The specimens for the experiments were modelled using finite elements with microstructural modeling and homogenization techniques.

The raster angle, the build orientation, and the infill density were found to be the principal factors that affected the elastic response of specimens. The results obtained indicated that the specimens with a 0° raster angle, parallel orientation to the loading direction, and high infill density presented the highest elastic modulus values [36]. Studies examined the effects of printing parameters on the mechanical properties of 3D-printed polymer composites/structures. Khan et al. [26] found for FFF-printed PLA-PETG-ABS composites that infill density and raster angle significantly impacted the tensile strength/modulus, with 100% infill and a 0° raster angle being optimal. Karimi et al. [36] analyzed the effect of the layer angle as well as the ambient temperature on the mechanical and fracture properties of unidirectional 3D-printed PLA materials. The study concluded that both the layer angle and the ambient temperature had major effects on the mechanical and fracture behavior of the specimens. Samples made with a 0° layer angle and tested at room temperature showed the highest tensile strengths and fracture toughness. These studies indicate that the optimal values of these factors depend on the specific application of interest and the desired properties.

The novelty of this work lies in its comprehensive approach to evaluating the mechanical properties and fracture toughness of 3D-printed PLA composites reinforced with chopped carbon fibers. Unlike previous studies that primarily focused on continuous carbon fibers, this research investigates the effects of chopped fibers, which offer distinct advantages in terms of processing and material behavior. This study aims to fill the gap in the literature by providing detailed insights into the performance enhancements achievable through the use of chopped carbon fibers in PLA matrices, thereby advancing the potential applications of 3D-printed composites in engineering fields.

The motivation for studying PLA composites with chopped carbon fibers stems from the need to enhance the mechanical properties of PLA for broader engineering applications.

PLA's biodegradability and ease of processing make it an attractive material; however, its inherent mechanical limitations restrict its use in high-performance applications. By incorporating chopped carbon fibers, we aim to leverage their high strength-to-weight ratio and excellent stiffness to create a composite material that combines the environmental benefits of PLA with the superior mechanical properties of carbon fibers. This study not only provides a sustainable solution but also extends the application range of 3D-printed PLA composites.

This study aimed to investigate the effect of chopped carbon fibers on the mechanical properties and fracture toughness of PLA 3D-printed parts. Specifically, the objectives were as follows:

1. To fabricate PLA-CF composite samples with varying CCF orientations (0° , $0^\circ/90^\circ$, $+45^\circ/-45^\circ$, and $0^\circ/+45^\circ/-45^\circ/90^\circ$) using the FFF technique.
2. To experimentally evaluate the tensile properties and fracture toughness (via the single-edge notched bend (SENB) method) of the composite samples.
3. To look at how in-plane raster orientation affects the tensile and fracture strengths of PLA parts made with the FDM method. (The paper starts with a theoretical background of the stress field around the crack tip.)
4. To develop and validate a finite element analysis (FEA) model using Abaqus to predict the fracture toughness of the composite samples.
5. To analyze the effects of CF orientation on the mechanical properties and fracture toughness of the PLA-CF composites.
6. To provide insights into the strengthening and toughening mechanisms of PLA-CF composites and their potential applications.

This study aims to contribute to the understanding of the mechanical behavior of PLA-CF composites fabricated via FFF, particularly the effects of CF orientation on fracture toughness. By employing both experimental and simulation approaches, this research seeks to provide a comprehensive analysis of the mechanical performance of these composites and their potential for structural applications.

The rest of this paper is organized as follows. Section 2 defines the materials and experimental methods used. These include the PLA and carbon fiber materials, details of the composite fabrication procedure through the FFF process, the mechanical testing methodologies (tensile and fracture toughness), and the FEA modeling approach. In Section 3, the obtained results, such as the tensile properties, the values of fracture toughness, the fractographic analysis, and the mechanisms of strengthening and toughening, along with a comparison with earlier studies, are discussed. Section 4 summarizes the major conclusions and practical implications, as well as future research directions.

2. Theoretical Background

The theoretical framework underpinning fracture mechanics analysis is essential for interpreting the experimental findings and comprehending the fracture behavior of the composite samples. In the realm of linear elastic fracture mechanics (LEFM), the stress field near the crack tip in a linear elastic material subjected to mode I loading can be defined by the following equation [37]:

$$\begin{aligned}\sigma_{rr} &= \frac{K_I}{\sqrt{2\pi r}} \left[\frac{5}{4} \cos\left(\frac{\theta}{2}\right) - \frac{1}{4} \cos\left(\frac{3\theta}{2}\right) \right] + \dots \\ \sigma_{\theta\theta} &= \frac{K_I}{\sqrt{2\pi r}} \left[\frac{3}{4} \cos\left(\frac{\theta}{2}\right) + \frac{1}{4} \cos\left(\frac{3\theta}{2}\right) \right] + \dots \\ \sigma_{r\theta} &= \frac{K_I}{\sqrt{2\pi r}} \left[\frac{1}{4} \sin\left(\frac{\theta}{2}\right) + \frac{1}{4} \sin\left(\frac{3\theta}{2}\right) \right] + \dots\end{aligned}\quad (1)$$

where σ_{ij} represents the stress tensor components, r and θ are the polar coordinates centered at the crack tip, K_I is the mode I stress intensity factor that quantifies the magnitude of stress around the crack tip, and $f_{ij}(\theta)$ is a dimensionless function of the angle θ . It is important to note that while Equation (1) is accurate for isotropic materials, it can still serve as a

good approximation for linear elastic stresses near the crack tip for materials exhibiting slight anisotropic behavior [38]. According to the principles of LEFM, mode I fracture occurs when the stress intensity factor, K_I , reaches its critical value, K_{Ic} , which is defined as the material's fracture toughness [37]. However, when the amount of plastic deformation around the crack tip is not negligible, the assumption of linear elasticity breaks down and an alternative characterizing parameter, J , is employed. The J -integral, proposed by Rice [39], represents the rate of change in the net potential energy for non-linear elastic solids and serves as a parameter quantifying the singularity strength at the crack tip in elastic–plastic fracture mechanics.

The J -integral is defined as follows:

$$J = \int_{\Gamma} (W dy - T_i \partial u_i / \partial x \partial s) \quad (2)$$

where W is the strain energy density, T_i is the traction vector, u_i is the displacement vector, and Γ is a counterclockwise integration path surrounding the crack tip [37,38]. The J -integral provides a measure of the energy release rate associated with crack growth and is particularly useful for materials exhibiting significant plastic deformation at the crack tip. In the context of this study, both the stress intensity factor (K_I) and the J -integral will be employed to characterize the fracture behavior of the PLA-CF composite samples, depending on the level of plastic deformation observed. The theoretical background provided by LEFM and elastic–plastic fracture mechanics will guide the interpretation of experimental data and facilitate a comprehensive understanding of the fracture toughness of the composites under investigation.

3. Materials and Methods

3.1. Materials

In this work, the following components were utilized: PLA granules and short carbon fibers (CCFs) of polyacrylonitrile (PAN), which were all acquired commercially from Dongguan ANT Plastic Technology Co., Ltd., Dongguan, China. The CCFs had diameters in the range of 40–60 μm and lengths in the range of 15–20 μm , as recommended for better reinforcement of the polymer composites [40]. Before mixing the polymer components, the carbon fibers' surfaces were treated to improve their interfacial bonding with the PLA matrix. The CCFs were placed in a solution of 20 wt% H_2SO_4 so that oxygen-attached functional groups could develop on the surface, enhancing wettability and achieving greater surface rugosity for better interfacial bonding [41]. In addition, to improve the performance properties of PLA and the PLA/CCF filaments, the CCFs were coated with a KH570 saline coupling agent (γ -aminopropyltriethoxysilane). Silane coupling agents are widely used to enhance interfacial adhesion between reinforcing fibers and polymeric matrices. The processing was performed using a TY-7004 single-screw extrusion machine obtained from Dongguan Tienyu Machinery Co., Ltd., China. The extrusion was performed at a temperature of 180 $^{\circ}\text{C}$ and a screw speed of 200 revolutions per minute. These parameters were set based on general recommendations for PLA processing [42]. The quantity of carbon fiber in the PLA/CCF filaments was 15 wt%—a common value in chopped fiber-reinforced PLA composites. The filaments were extruded to a diameter of 1.75 mm—a standard size for FDM printers [24]. To ensure precise control of the filament diameter, a diameter measurement system was incorporated into the extruder. This system continuously monitored the filament during production, automatically adjusting the extrusion parameters to maintain a consistent diameter of 1.75 mm. Real-time feedback and adjustments were made to correct any deviations, ensuring uniform filament dimensions essential for high-quality 3D printing. Figure 1 schematically describes the reinforcement mechanism of the PLA composite samples with the incorporation of CCF.

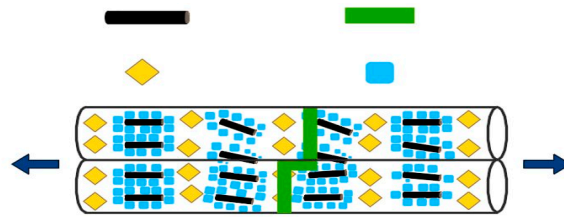


Figure 1. Reinforcement mechanism of carbon fibers in PLA.

3.2. Composite Fabrication

The composite samples were fabricated using the fused deposition modeling (FDM) technique, also referred to as fused filament fabrication (FFF), with a Creality Ender 3 Pro 3D printer (Creality, Shenzhen, China). Initially, a 3D model was created in SolidWorks software 2017, which was then converted into an STL format file. This STL file was processed by slicing software specific to (AM) technology, which divided the model into layers and generated a file containing the necessary information for each layer, including toolpath coordinates and extrusion rates. The slicing data were subsequently translated into machine instructions using G-code.

During the manufacturing process, the filament was heated to a printing temperature of 200 °C and extruded through a nozzle with a diameter of 0.4 mm to print each layer of the object. After each layer was printed, the nozzle moved vertically according to a predetermined layer height to begin printing the next layer. The slicing software defined the filament trajectory to fill the product geometry and create a shell with a specific raster angle pattern, which was achieved by alternating the orientation of successive layers. To address the challenge of printing with a high fiber content using a 0.4 mm nozzle, a heated chamber was utilized, and the filament was pre-heated to a molten state before extrusion in the production process, as shown in Figure 2. The platform temperature was maintained at 50 °C to mitigate residual stress, facilitating smoother extrusion and preventing nozzle clogging, thus enabling the successful fabrication of PLA/CCF samples with enhanced mechanical properties.

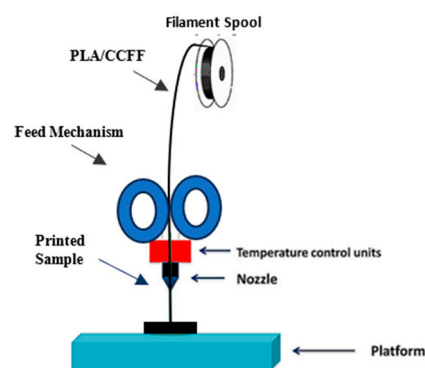


Figure 2. The production process for the samples.

The following sample groups were used to investigate the influence of fiber orientation, the composite samples being fabricated with four different fiber orientations: 0°, 0°/90°, +45°/−45°, and 0°/+45°/−45°/90°. These orientations were achieved by controlling the filament deposition pathways during the printing process via the slicing software. The 0° orientation indicates that all layers were printed with the fibers aligned along the primary loading direction, while the 0°/90° orientation alternated between 0° and 90° fiber orientations in successive layers. The +45°/−45° orientation alternated between +45° and −45° fiber orientations, and the 0°/+45°/−45°/90° orientation combined all three orientations in a specific sequence [34]. For each orientation group, a sufficient number of samples were printed to ensure statistical significance in the subsequent mechanical testing.

The critical printing parameters employed for fabricating the PLA-CCF composite samples via the FDM process are summarized in Table 1. These parameters, including printing speed, nozzle diameter, layer thickness, raster angle, and print temperature, were carefully selected based on prior optimization studies to ensure consistent and high-quality printing. Table 2 outlines the different composite sample groups produced, each characterized by a distinct fiber orientation configuration (0° , $0^\circ/90^\circ$, $+45^\circ/-45^\circ$, and $0^\circ/+45^\circ/-45^\circ/90^\circ$). The dimensions of the printed specimens, tailored for subsequent mechanical testing and fracture toughness evaluation, are also specified in Table 2.

Table 1. Technical parameters for manufacturing polylactic acid carbon fiber-reinforced samples.

Parameters	Value
Printing speed (mm/s)	60
Nozzle diameter (mm)	0.4
Layer thickness (mm)	0.2
Supplied speed (mm/s)	60
Print temperature ($^\circ\text{C}$)	200
Infill ratio	100%

Table 2. Composite sample groups with different fiber orientations.

Sample Group	Raster Orientation	Description
A ₁	0°	All layers are printed with fibers aligned along the primary loading direction
A ₂	$0^\circ/90^\circ$	Alternating layers with fibers oriented at 0° and 90°
A ₃	$+45^\circ/-45^\circ$	Alternating layers with fibers oriented at $+45^\circ$ and -45°
A ₄	$0^\circ/+45^\circ/-45^\circ/90^\circ$	Layers with fibers oriented at 0° , $+45^\circ$, and 90° in a specific sequence

The comprehensive experimental workflow, encompassing sample fabrication and the various testing procedures, is illustrated in Figure 3. This diagram provides a step-by-step overview of the entire process, starting from the preparation of the 3D printer to the loading of the PLA/CCF filament. The 3D printing process, including the manufacturing of samples with different orientations of the fibers, was followed by sample preparation steps, including cutting samples into the required shape and size and making notches on the samples for fracture toughness tests. Other stages included performing tensile tests according to ASTM standards, from which load–displacement data could be extracted, and the evaluation of fracture toughness using the SENB method. The final steps included analysis of the data, where the acquired mechanical properties were interpreted, the fracture toughness values were calculated, and the effect of fiber orientation on the composite’s performance was investigated.

3.2.1. Tensile Testing

Uniaxial tensile tests were conducted using an Instron 5980 system, operating at a crosshead speed of 1 mm/min in accordance with ASTM D638 procedures [43–45]. Dog-bone specimens, prepared following the ASTM D638 Type IV standard, were subjected to tension testing. The average maximum tensile strength, elastic modulus, and elongation at break were calculated based on results obtained from three specimens per group [46]. This approach ensured consistency with established testing methodologies, thereby facilitating reliable comparison and reproducibility of the results. The use of the ASTM D638 standard, despite its primary application to unreinforced plastics, is justified by its widespread recognition and detailed procedural guidelines, which are applicable to composite materials as well.

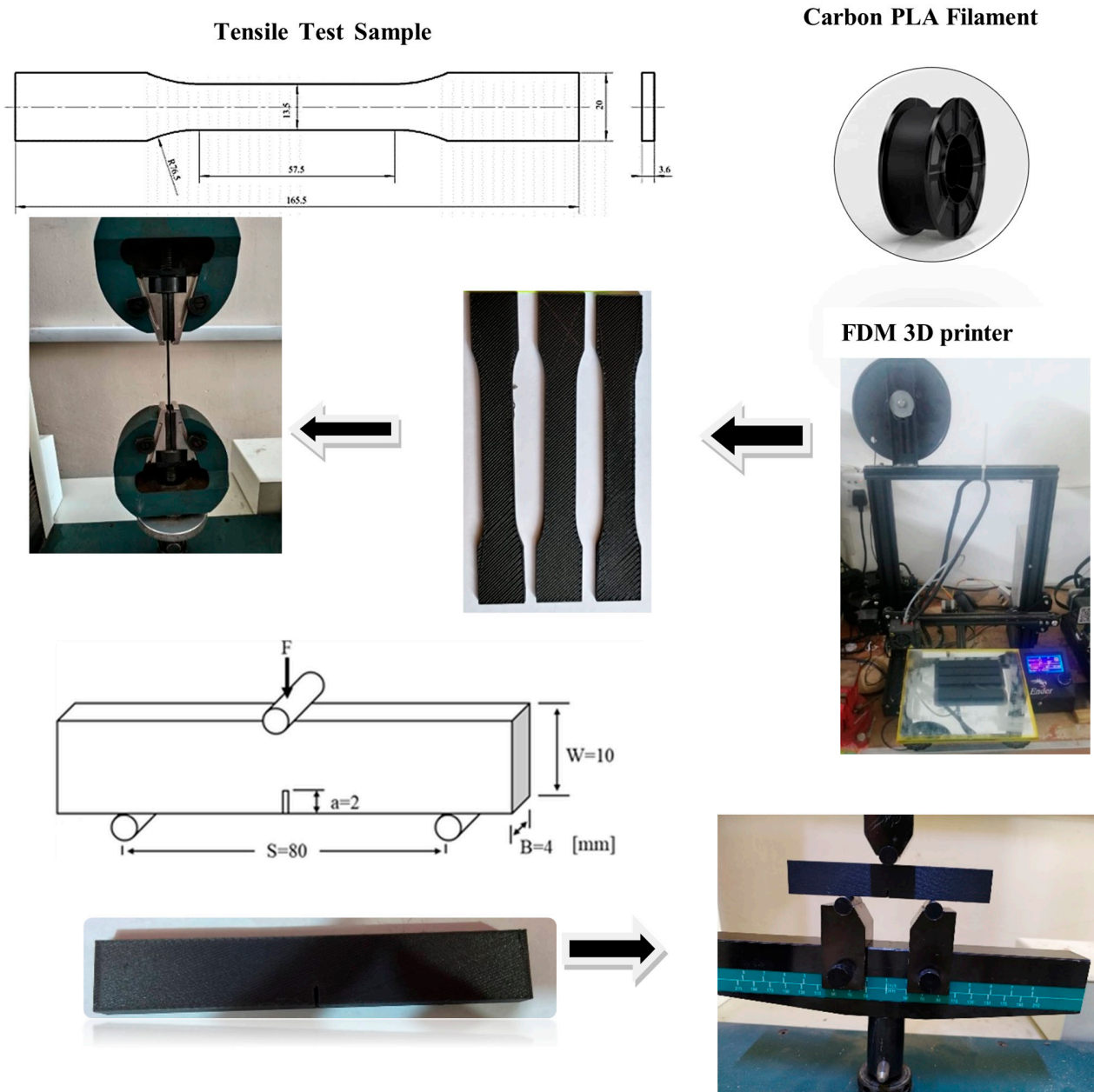


Figure 3. Sample fabrication and testing process for the experiment.

3.2.2. Fracture Testing for Mode I

The fracture toughness of the SENB samples was evaluated under three-point bending on an Instron 5980 system. The samples were loaded at a rate of 0.5 mm/min until failure [47,48]. The K_{IC} critical stress intensity factor was determined on the basis of the maximum load measured for each raster pattern. The K_{IC} could be obtained using the equation below.

$$K_{IC} = \frac{P_{max}}{BW^{1/2}} f\left(\frac{a}{W}\right)$$

where P_{max} is the maximum load recorded during the test (N), B is the thickness of the specimen (mm), W is the width of the specimen (mm), and a is the initial crack length (mm). The function $f\left(\frac{a}{W}\right)$ is a dimensionless geometry factor that depends on the ratio of the crack length to the specimen width and can be determined from standard tables or empirical equations.

4. Finite Element Analysis

The finite element analysis (FEA) was performed using the commercial software Abaqus (version 2017; Dassault Systèmes, Providence, RI, USA) to predict the fracture toughness values of the PLA-CCF composite samples. A three-dimensional (3D) model of the single-edge notched bend (SENB) specimen geometry was created based on the experimental dimensions as shown in Figure 4 and material defined from specified in Table 2. The SENB specimen was discretized using a structured mesh of hexahedral elements with a higher mesh density in the crack-tip region to capture the stress singularity accurately. Convergence studies were performed to ensure that the mesh size did not significantly influence the fracture toughness predictions. The PLA-CCF composite was modelled as a transversely isotropic material, with the material properties defined using the elastic constants and strengths obtained from experimental characterization and data reported in the literature [43,44]. The carbon fibers were assumed to be aligned in the specified orientations (0° , $0^\circ/90^\circ$, $+45^\circ/-45^\circ$, and $0^\circ/+45^\circ/-45^\circ/90^\circ$) within the PLA matrix.

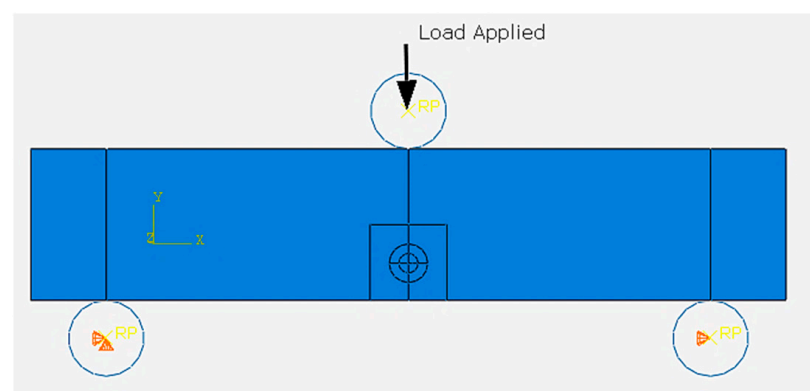


Figure 4. The applied load and the boundary condition.

The boundary conditions were applied to replicate the three-point bend configuration used in the experimental SENB tests. The bottom surface of the specimen was constrained in the vertical direction, while the loading was applied through a prescribed displacement on the top surface at the midspan location.

The crack was modelled as a seam crack with an initial crack length equal to the notch length introduced during sample preparation. The crack tip was defined as a focused circular region with a radius of 2 mm, consistent with the experimental observations.

A mesh sensitivity study was conducted to quantify the degree of discretization required for the convergence of the finite element solutions [49,50]. This was achieved by systematically varying the number of elements in the SENB model and evaluating the response. Models were generated with total element counts ranging from 2000 to 16,000 two-dimensional 8-noded quadrilateral elements (CPS8) as shown in Figure 5. All other parameters, including geometry, material properties, loads, and boundary conditions, were kept constant.

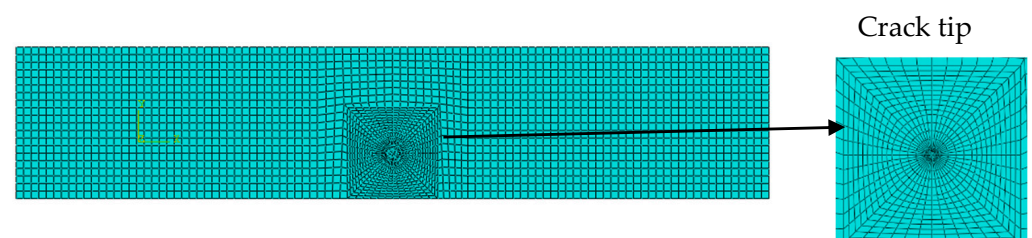


Figure 5. The generated mesh.

Prediction of Fracture Toughness Values

The fracture toughness predictions were based on the J-integral approach, which is suitable for materials exhibiting significant plastic deformation at the crack tip. The J-integral was evaluated along a contour integral path surrounding the crack tip, and the critical value of the J-integral at fracture initiation was determined. The critical J-integral value (J_c) was then used to calculate the fracture toughness (K_{IC}) using the following equation [37]:

$$K_{IC} = \sqrt{E * J_c} \quad (3)$$

where E is the effective elastic modulus of the PLA-CCF composite, which accounts for the anisotropic behavior of the material.

The FEA simulations were performed for each fiber orientation group, and the predicted fracture toughness values were compared with the experimental results. The influence of fiber orientation on fracture toughness was analyzed, and the mechanisms governing the fracture behavior of the PLA-CCF composites were investigated. Additionally, the stress and strain distributions within the composite samples were examined to gain insights into the failure mechanisms and the role of fiber reinforcement in enhancing fracture toughness.

5. Results and Discussion

5.1. Tensile Properties

The tensile stress–strain curves obtained from the uniaxial tensile tests on the PLA-CCF composite samples are presented in Figure 6. The curves exhibit a typical elastoplastic behavior, with an initial linear elastic region followed by a non-linear plastic deformation region until failure. The results indicate a significant improvement in tensile properties with the incorporation of chopped carbon fibers (CCFs) into the PLA matrix, corroborating findings from previous studies [9,10].

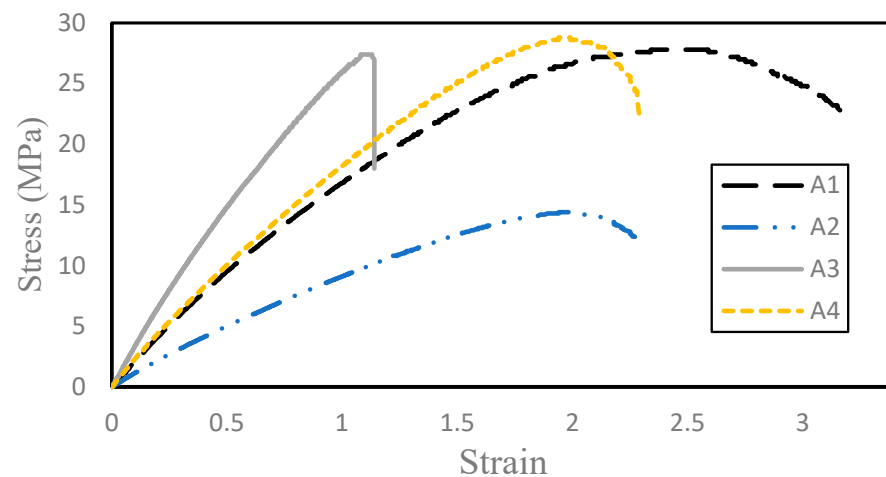


Figure 6. The stress–strain curves for the samples.

The tensile strength and elastic modulus values of the PLA-CCF composites for different fiber orientations are presented in Figure 6. As evident observed from the Figure 7, the incorporation of chopped carbon fibers (CCFs) into the PLA matrix resulted in significant improvements in tensile properties compared to unreinforced PLA. The 0° fiber orientation (sample A1) exhibited a tensile strength of 27.8 MPa, benefiting from the fibers being aligned along the loading direction, which effectively transferred the applied loads. Similarly, sample A3, another 0° -oriented sample, showed a high tensile strength of 27.4 MPa.

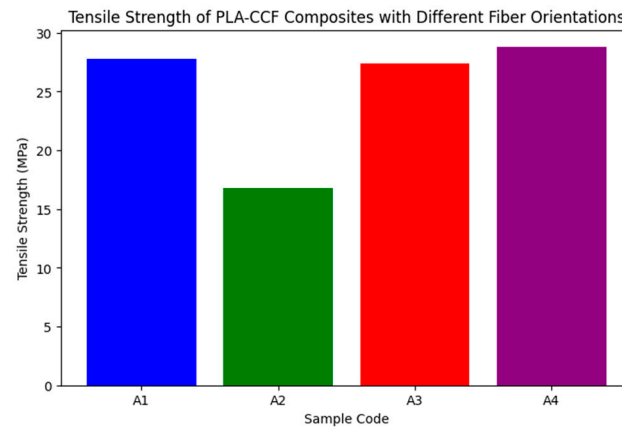


Figure 7. Tensile strength of PLA-CCF composites with different fiber orientations.

In contrast, the $0^\circ/90^\circ$ orientation (sample A2) displayed a lower tensile strength of 16.786 MPa, suggesting that while fibers oriented perpendicularly to the loading direction can still contribute to load bearing, their efficiency is reduced compared to unidirectional alignment. Sample A4, with a tensile strength of 28.8 MPa, outperformed the other orientations, indicating that the specific distribution and arrangement of fibers in this sample facilitated superior mechanical performance.

The variation in tensile strengths among the different fiber orientations highlights the anisotropic nature of the composite material. The fibers' ability to transfer and absorb applied loads effectively depends significantly on their orientation within the matrix. This anisotropic behavior is crucial in designing composite materials for specific engineering applications where directional strength and stiffness are paramount.

In summary, the study underscores the importance of fiber orientation in enhancing the mechanical properties of PLA-CCF composites. Aligning fibers along the primary load direction maximizes tensile strength and modulus, making these composites more suitable for high-performance applications requiring specific mechanical characteristics.

5.2. Fracture Toughness Values from SENB Testing

The fracture toughness values obtained from the single-edge notched bend (SENB) tests are presented in Figure 8, and Table 3 shows the load–displacement curves of the samples. The results demonstrate that the incorporation of chopped carbon fibers (CCFs) significantly enhanced the fracture toughness of the PLA composites compared to unreinforced PLA.

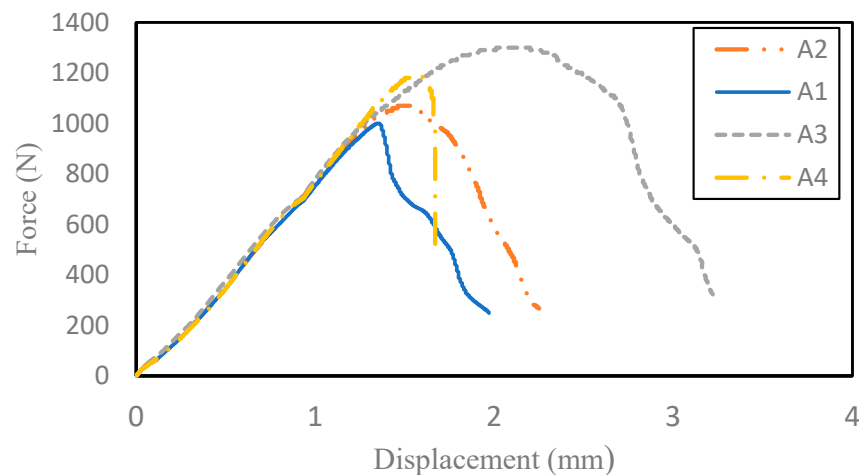


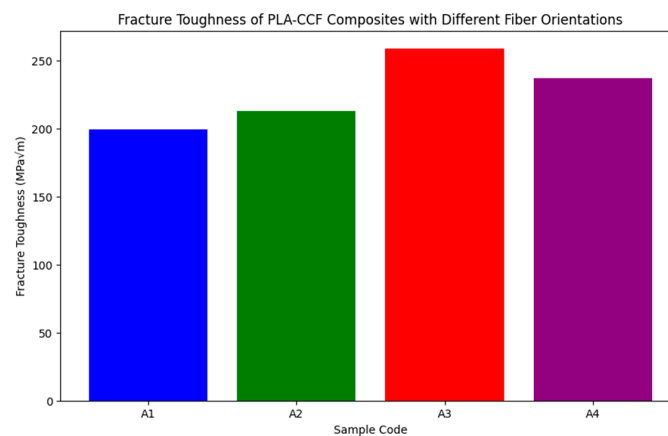
Figure 8. The SENB load–displacement results for the samples.

Table 3. Fracture loads and fracture toughness (K_{IC}) values for different SENB specimens.

Sample	Max. Fracture Loads (N)	K_{IC} (MPa $\sqrt{\text{m}}$)
A1	1000	199.34
A2	1072	213.28
A3	1300	259.12
A4	1190	237.21

The load–displacement curves (Figure 8) and the corresponding fracture toughness values (Table 3) reveal that the $0^\circ/+45^\circ/-45^\circ/90^\circ$ fiber orientation exhibited the highest fracture toughness, followed by the $+45^\circ/-45^\circ$ orientation. This trend can be attributed to the combined effects of fiber bridging, crack deflection, and fiber pull-out mechanisms, which enhance energy dissipation and crack growth resistance.

The significant improvement in fracture toughness with the incorporation of CCF underscores the effectiveness of fiber reinforcement in enhancing the mechanical properties of PLA composites can be observed that in Figure 9.

**Figure 9.** Fracture toughness of different samples.

The chopped carbon fibers provide a high strength-to-weight ratio, excellent stiffness, and thermal stability, which contribute to their ability to improve fracture toughness. These properties allow the fibers to effectively transfer and absorb applied loads, preventing crack propagation and increasing the material's resistance to fracture [51].

The orientation of the fibers played a crucial role; among the different fiber orientations, the samples with a $0^\circ/+45^\circ/-45^\circ/90^\circ$ orientation exhibited the highest fracture toughness values, followed by the $+45^\circ/-45^\circ$ orientation. This behavior can be attributed to the combined effects of fiber bridging, crack deflection, and fiber pull-out mechanisms that contribute to enhanced energy dissipation and crack growth resistance. Similar observations were made by Ayatollahi et al. [34], who reported that the fracture strengths of 3D-printed PLA specimens were influenced by the raster angle (fiber orientation), with the highest fracture strengths being observed for specimens with a $0^\circ/90^\circ$ raster angle. The fracture loads obtained from the SENB tests, along with the corresponding fracture toughness values, are shown in Figure 6. The fracture loads follow a similar trend to the fracture toughness values, with the highest loads observed for the $0^\circ/+45^\circ/90^\circ$ and $+45^\circ/-45^\circ$ orientations.

5.3. Analysis of Effects of Fiber Orientation on Properties

The variations in tensile performance and fracture toughness can be explained by the different fiber orientations and their effect on load transfer and failure mechanisms within the composite. In the 0° orientation, the fibers are aligned along the loading direction

to effectively transfer the applied load, increasing the composite's strength and rigidity. However, this leads to a limitation in ductility and fracture toughness due to the lack of fiber bridging and crack deflection mechanisms. In contrast, the $+45^\circ/-45^\circ$ and $0^\circ/+45^\circ/90^\circ$ orientations distribute the fibers in multiple directions, promoting more effective crack deflection, fiber bridging, and fiber pull-out mechanisms. These mechanisms contribute to increased energy dissipation and crack growth resistance, leading to improved fracture toughness. According to the results reported in Table 3 the best mechanical properties, including tensile strength, elongation at break, and fracture toughness, were obtained by the specimens oriented in the $+45^\circ/-45^\circ$ printing direction.

Similar results were reported by Oviedo et al. [52] and Jap et al. [53] for the tensile behavior and fatigue performance of parts produced by the FDM technique with PLA. Oviedo et al. showed that the strain to failure of parts additively manufactured from PLA with a $+45^\circ/-45^\circ$ printing direction was about 50% higher than those additively manufactured with a $0^\circ/90^\circ$ printing direction. On the other hand, dealing with fatigue performance, also in the study [53] reported that, for a constant stress amplitude, the number of cycles to failure for samples with a $+45^\circ/-45^\circ$ raster orientation was more than twice that of the $0^\circ/90^\circ$ raster orientation. The fact that the tensile properties and the fracture toughness values were found to be anisotropic shows the need to include fiber orientation in such analyses and, in order to assure the best performance of PLA-CCF composites in different applications, an optimization of the single directivity orientation.

5.4. Microscopic Examination of Fracture Surfaces

Scanning electron microscopy (SEM) analysis was conducted to investigate the fracture surfaces of the PLA-CCF composite samples and gain insights into the failure mechanisms. Figure 10 shows an SEM micrograph of the chopped carbon fibers dispersed within the PLA matrix. The image was captured at a magnification of $891\times$, with an accelerating voltage of 20.00 kV and a working distance of 2.768 mm. The scale bar indicates a length of 50 micrometers (μm). Several carbon fibers with varying diameters can be observed, indicated as D1 (21.6 μm), D2 (9.36 μm), D3 (8.15 μm), and D4 (18.09 μm). The distribution and orientation of the chopped carbon fibers within the PLA matrix play a crucial role in determining the composite's mechanical properties, including tensile strength, modulus, and toughness. In this micrograph, the fibers appear randomly oriented and non-uniformly distributed, which is typical for short-fiber-reinforced composites. The dispersion and orientation of the fibers can significantly influence the composite's performance, as aligned fibers generally provide better mechanical properties along the alignment direction. In comparison, random dispersion can lead to more isotropic properties.

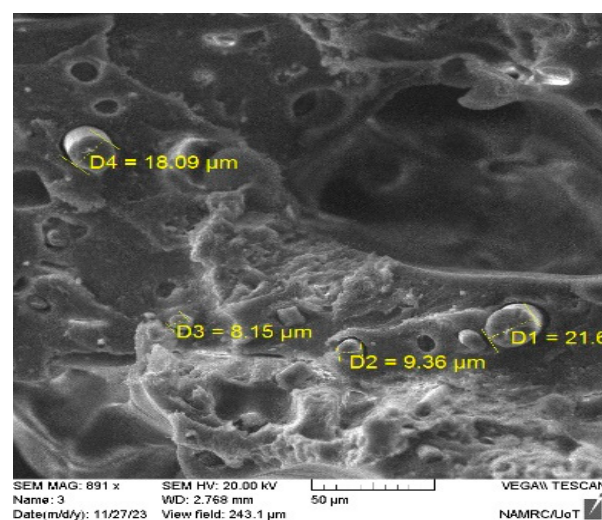


Figure 10. SEM of PLA reinforced by CCF.

The distribution of the chopped carbon fibers in the PLA matrix is a critical factor in determining the composite material's mechanical properties, such as tensile strength, modulus, and toughness. In this image, the fibers appear to be randomly oriented and not uniformly distributed, which is typical for short-fiber-reinforced composites. The dispersion and orientation of the fibers can significantly affect the composite's performance, as aligned fibers generally provide better mechanical properties in the direction of alignment, while random dispersion can lead to more isotropic properties.

Figure 11 presents an SEM micrograph of the fracture surface of a tensile specimen from Group 1, which has a 0° fiber orientation. The image reveals slight air gaps between the filaments—an inherent feature of 3D-printed specimens. Notably, the bonding lines between the filaments do not contribute significantly to energy dissipation during fracture, as evidenced by the presence of only minor damage zones in these regions.

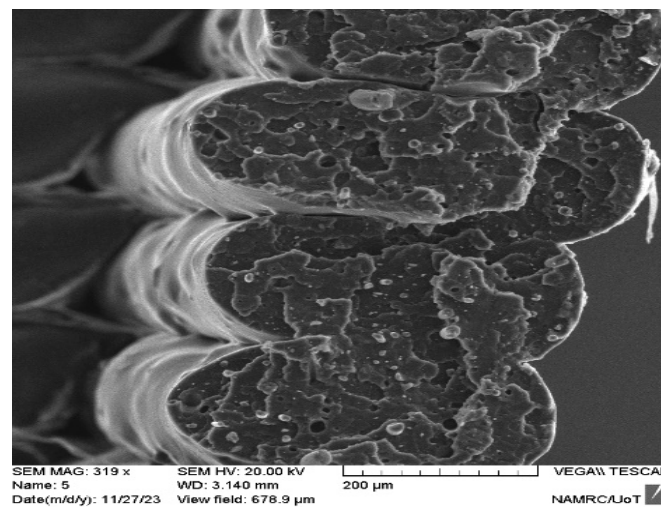


Figure 11. Fracture surface of samples.

The SEM analysis provided valuable information on the fracture mechanisms of the 3D-printed materials and their effect on mechanical properties and performance. Hence, the importance of considering fiber orientation and other intrinsic features of 3D-printed materials in designing and analyzing components for a specific application is brought into perspective. The micrograph of the fracture surface suggests that the adhesion between filaments is less perfect, which will influence the mechanical properties of the material. These small damage zones in the bonding lines suggest that the strength of the bonding is very weak in relation to dissipating energy during fracture; hence, crack propagation may result along these lines. The fiber orientation can affect the fracture mechanism of the specimen. A $+45^\circ/-45^\circ$ -oriented specimen will have different fracture behavior to a $0/90^\circ$ -oriented specimen. The differences between the SEM micrographs accentuate how the fiber orientation influences the mechanical properties and performance of a 3D-printed material. These results are in good agreement with those obtained by [54,55], in which it was found that the bonding in 3D-printed PLA samples did not make a high contribution to the fracture energy. In general, SEM imagery has offered invaluable data in comprehending the fracture mechanisms of 3D-printed materials. Their influence on mechanical properties and performance as well as fiber orientation and other intrinsic features of 3D-printed materials have to be considered in designing and analyzing components for specific applications.

5.5. Finite Element Analysis Results

FEA was performed for each fiber orientation group, and the predicted fracture toughness values were compared with the experimental results. The association between the FEA results and the experimental data was mostly satisfactory, and the model represented the trends and fracture toughness for the various fiber orientations [56,57]. The data from

the FEA, together with the outcomes of the experiment, gave an insight into the toughening and strengthening mechanisms of the PLA-CCF composites.

Stress Distribution and Crack-Tip Fields

The FEA model enabled the visualization and analysis of the stress distribution and crack-tip fields within the SENB specimens. Figure 12 shows a contour plot of the von Mises stress distribution for sample A1, representing the 0° fiber orientation. For the A1 sample, the highest stress was at the crack tip, as expected. The distribution of stress ahead of the crack tip showed a signature pattern because of the crack-tip singularity, and the maximum occurred at the crack and then decayed radially outwards. Crack-tip stress fields were determined using the J-integral approach, which is adequate for materials undergoing large plastic deformation at the tip of the crack.

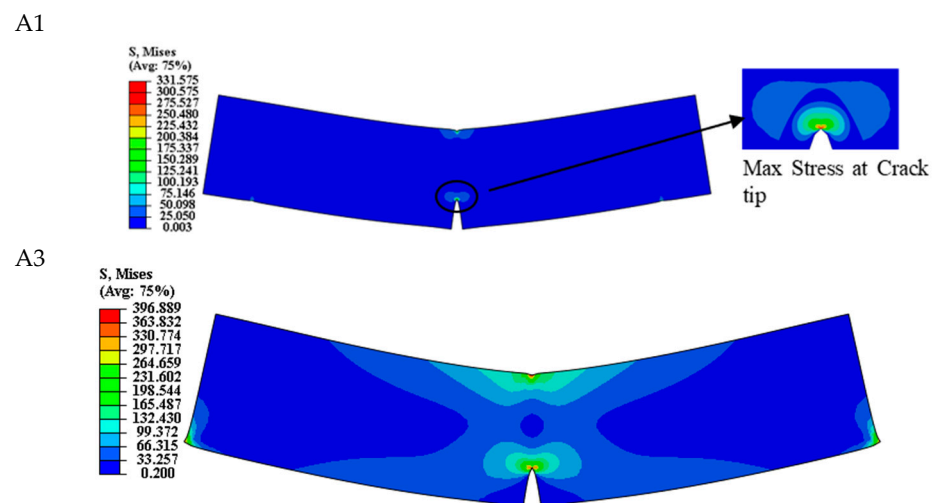


Figure 12. Von Mises stress distribution and crack-tip fields obtained from FEA simulations for the A1 and A3 samples.

Using a contour integral path surrounding the crack tip, the J-integral was evaluated, and the critical value of the J-integral at fracture initiation (J_c) was determined. The critical value of the J-integral (J_c) was used to calculate the value of the fracture toughness (K_{Ic}) through the following expression: $K_{Ic} = \sqrt{E^* J_c}$, where E is the effective elastic modulus of the material undergoing fracture and takes into account the anisotropic behavior of the material. It is obvious that the FEA simulations proved that ghost elements exist, as did the prevention of cracking and the closely related stress distributions and crack-tip fields responsible for the fracture behavior of the PLA-CCF composites to a great extent. The predictions of the FEA model were in very good agreement with the experimental data, accurately capturing the trends and relative differences in fracture toughness associated with the several fiber orientations. The J-integral approach, combined with the transversely isotropic material model and adequate boundary conditions, allowed reliable fracture behavior predictions of the PLA-CCF composites. In general, the results of this investigation reveal the high potential for PLA-CCF composites as really high-performance materials with very good feasibility for obtaining tailored mechanical properties, especially fracture toughness, by the proper selection of fiber orientations. These findings enrich the research on the development of advanced composite materials intended for several structural and functional applications.

6. Conclusions

The present study documents a systematic investigation into the influence of chopped carbon fiber (CCF) reinforcement and fiber orientation on the tensile strength and fracture toughness of 3D-printed PLA. The key achievements of this study include the following:

- Enhanced tensile strength:
 - The incorporation of CCF reinforcement resulted in a significant enhancement in tensile strength compared to unreinforced PLA (27.8 MPa).
 - The $0^\circ/+45^\circ/90^\circ$ fiber orientation (sample A4) exhibited the highest tensile strength of 28.8 MPa, representing a 3.6% improvement over the unreinforced baseline.
 - Conversely, the $0^\circ/90^\circ$ orientation (sample A2) displayed a 39.6% decrease in tensile strength (16.786 MPa), highlighting the profound impact of fiber orientation on tensile properties.
- Improved fracture toughness:
 - The fracture toughness data revealed a trend where multi-directional fiber orientations outperformed unidirectional orientations.
 - The $+45^\circ/-45^\circ$ orientation (sample A3) yielded the maximum fracture toughness of 259.12 MPa $\sqrt{\text{m}}$ —a remarkable 29.9% increase compared to unreinforced PLA (199.34 MPa $\sqrt{\text{m}}$).
 - The $0^\circ/+45^\circ/90^\circ$ orientation (sample A4) exhibited an 18.9% improvement in fracture toughness (237.21 MPa $\sqrt{\text{m}}$), while the $0^\circ/90^\circ$ orientation (sample A2) showed a modest 7.0% increase (213.28 MPa $\sqrt{\text{m}}$).
- Critical role of fiber orientation:
 - The study underscores the critical role played by fiber orientation in tailoring the mechanical properties of CCF-reinforced PLA composites.
 - Unidirectional fiber orientations, such as 0° , enhance tensile strength through efficient load transfer.
 - Multi-directional orientations facilitate improved fracture toughness by promoting mechanisms like crack deflection, fiber bridging, and fiber pull-out.
 - The observed inverse correlation between tensile strength and fracture toughness highlights the importance of judiciously selecting the fiber orientation to meet specific mechanical performance requirements.
- Optimizing composite architectures:
 - Composite designers can leverage the trade-off between tensile strength and fracture toughness to optimize the desired combination of strength, stiffness, and fracture resistance by strategically tailoring composite architectures.
- Future research directions:
 - Future research endeavors should focus on further exploring the underlying mechanisms governing the observed trends, potentially through in-depth microstructural and fractographic analyses.
 - Investigating the effect of varying fiber content and aspect ratios could provide valuable insights for optimizing the mechanical performance of CCF-reinforced PLA composites.

This study contributes to the rapidly evolving field of additive manufacturing by demonstrating the potential of CCF reinforcement and strategic fiber orientation in enhancing the mechanical properties of 3D-printed PLA composites. The findings pave the way for the development of high-performance, sustainable, and lightweight composite materials for a wide range of structural and functional applications, aligning with the principles of eco-friendly and resource-efficient manufacturing.

Author Contributions: Conceptualization, A.A.F.O., M.S.K. and E.K.N.; Methodology, A.A.F.O.; Software, A.A.F.O. and M.S.K.; Validation, A.A.J., E.K.N., L.A.A.-H., M.N.H. and E.S.A.-A.; Resources, L.A.A.-H. and M.N.H.; Writing—original draft, A.A.F.O.; Writing—review and editing, A.A.J.; Visualization, A.B., Z.T.A.-S. and E.S.A.-A.; Project administration, A.A.J.; Funding acquisition, A.B. and Z.T.A.-S. All authors have read and agreed to the published version of the manuscript.

Funding: This research received no external funding.

Data Availability Statement: The datasets generated and/or analyzed during the current study are available from the corresponding author upon reasonable request.

Acknowledgments: The authors wish to thank Mustansiriyah University (College of Engineering) and the University of Technology, Iraq, for the use of facilities in their labs. Thanks also to both Warith Al-Anbiyaa University, Iraq, and Al Hikma University College, Baghdad, Iraq.

Conflicts of Interest: The authors have no conflicts of interest to declare. All co-authors have seen and agree with the contents of this manuscript, and there are no financial interests to report.

References

1. Ngo, T.D.; Kashani, A.; Imbalzano, G.; Nguyen, K.T.Q.; Hui, D. Additive Manufacturing (3D Printing): A Review of Materials, Methods, Applications and Challenges. *Compos. Part B Eng.* **2018**, *143*, 172–196. [\[CrossRef\]](#)
2. Murariu, M.; Dubois, P. PLA composites: From production to properties. *Adv. Drug Deliv. Rev.* **2016**, *107*, 17–46. [\[CrossRef\]](#)
3. Gao, W.; Zhang, Y.; Ramanujan, D.; Ramani, K.; Chen, Y.; Williams, C.B.; Wang, C.C.L.; Shin, Y.C.; Zhang, S.; Zavattieri, P.D. The status, challenges, and future of additive manufacturing in engineering. *Comput.-Aided Des.* **2015**, *69*, 65–89. [\[CrossRef\]](#)
4. Thompson, M.K.; Moroni, G.; Vaneker, T.; Fadel, G.; Campbell, R.I.; Gibson, I.; Bernard, A.; Schulz, J.; Graf, P.; Ahuja, B.; et al. Design for Additive Manufacturing: Trends, opportunities, considerations, and constraints. *CIRP Ann.* **2016**, *65*, 737–760. [\[CrossRef\]](#)
5. Rajpurohit, S.R.; Dave, H.K. Impact strength of 3D printed PLA using open source FFF-based 3D printer. *Prog. Addit. Manuf.* **2021**, *6*, 119–131. [\[CrossRef\]](#)
6. Kartikeyan, B.; Ponshanmugakumar, A.; Saravanan, G.; BharathGanesh, S.; Hemamalini, V. Experimental and theoretical analysis of FDM AM PLA mechanical properties. *Mater. Today Proc.* **2023**. [\[CrossRef\]](#)
7. Caminero, M.Á.; Chacón, J.M.; García-Plaza, E.; Núñez, P.J.; Reverte, J.M.; Becar, J.P. Additive Manufacturing of PLA-Based Composites Using Fused Filament Fabrication: Effect of Graphene Nanoplatelet Reinforcement on Mechanical Properties, Dimensional Accuracy and Texture. *Polymers* **2019**, *11*, 799. [\[CrossRef\]](#) [\[PubMed\]](#)
8. Erdaş, M.U.; Yildiz, B.S.; Yildiz, A.R. Crash performance of a novel bio-inspired energy absorber produced by additive manufacturing using PLA and ABS materials. *Mater. Test.* **2024**, *66*, 696–704. [\[CrossRef\]](#)
9. Ogaili, A.A.F.; Jaber, A.A.; Hamzah, M.N. Wind turbine blades fault diagnosis based on vibration dataset analysis. *Data Brief* **2023**, *49*, 109414. [\[CrossRef\]](#)
10. Farah, S.; Anderson, D.G.; Langer, R. Physical and mechanical properties of PLA, and their functions in widespread applications—A comprehensive review. *Adv. Drug Deliv. Rev.* **2016**, *107*, 367–392. [\[CrossRef\]](#)
11. Mohamed, O.A.; Masood, S.H.; Bhowmik, J.L. Optimization of fused deposition modeling process parameters: A review of current research and future prospects. *Adv. Manuf.* **2015**, *3*, 42–53. [\[CrossRef\]](#)
12. Gardan, J. Additive manufacturing technologies for polymer composites: State-of-the-art and future trends. In *Structure and Properties of Additive Manufactured Polymer Components*; Friedrich, K., Walter, R., Soutis, C., Advani, S.G., Fiedler, B., Eds.; Woodhead Publishing: Cambridge, UK, 2020; pp. 3–15. [\[CrossRef\]](#)
13. Koç, O.O.; Meram, A.; Çetin, M.E.; Öztürk, S. Acoustic properties of ABS and PLA parts produced by additive manufacturing using different printing parameters. *Mater. Test.* **2024**, *66*, 705–714. [\[CrossRef\]](#)
14. Erdaş, M.U.; Yıldız, B.S.; Yıldız, A.R. Experimental analysis of the effects of different production directions on the mechanical characteristics of ABS, PLA, and PETG materials produced by FDM. *Mater. Test.* **2024**, *66*, 198–206. [\[CrossRef\]](#)
15. Ghabezi, P.; Sam-Daliri, O.; Flanagan, T.; Walls, M.; Harrison, N.M.; Ghabezi, P.; Sam-Daliri, O.; Flanagan, T.; Walls, M.; Harrison, N.M. Circular economy innovation: A deep investigation on 3D printing of industrial waste polypropylene and carbon fibre composites. *Resour. Conserv. Recycl.* **2024**, *206*, 107667. [\[CrossRef\]](#)
16. Shirasu, K.; Yamaguchi, Y.; Hoshikawa, Y.; Kikugawa, G.; Tohmyoh, H.; Okabe, T. Micromechanics study of short carbon fiber-reinforced thermoplastics fabricated via 3D printing using design of experiments. *Mater. Sci. Eng. A* **2024**, *891*, 145971. [\[CrossRef\]](#)
17. Ghabezi, P.; Flanagan, T.; Walls, M.; Harrison, N.M. Degradation characteristics of 3D printed continuous fibre-reinforced PA6/chopped fibre composites in simulated saltwater. *Prog. Addit. Manuf.* **2024**, *9*, 1–14. [\[CrossRef\]](#)
18. Vălean, E.; Foti, P.; Razavi, S.M.J.; Berto, F.; Marşavina, L. Static and fatigue behavior of 3D printed PLA and PLA reinforced with short carbon fibers. *J. Mech. Sci. Technol.* **2023**, *37*, 5555–5559. [\[CrossRef\]](#)
19. Iragi, M.; Pascual-González, C.; Esnaola, A.; Lopes, C.; Aretxabaleta, L. Ply and interlaminar behaviours of 3D printed continuous carbon fibre-reinforced thermoplastic laminates; effects of processing conditions and microstructure. *Addit. Manuf.* **2019**, *30*, 100884. [\[CrossRef\]](#)
20. Li, Y.; Gao, S.; Dong, R.; Ding, X.; Duan, X. Additive Manufacturing of PLA and CF/PLA Binding Layer Specimens via Fused Deposition Modeling. *J. Mater. Eng. Perform.* **2018**, *27*, 492–500. [\[CrossRef\]](#)
21. Thirugnanasambandam, A.; Subramanian, M.; Prabhu, B.; Ramachandran, K. Development and comprehensive investigation on PLA / carbon fiber reinforced PLA based structurally alternate layered polymer composites. *J. Ind. Eng. Chem.* **2024**, *136*, 248–257. [\[CrossRef\]](#)

22. Nanni, A.; Parisi, M.; Colonna, M.; Messori, M. Thermo-Mechanical and Morphological Properties of Polymer Composites Reinforced by Natural Fibers Derived from Wet Blue Leather Wastes: A Comparative Study. *Polymers* **2021**, *13*, 1837. [[CrossRef](#)] [[PubMed](#)]
23. Ramesh, P.; Prasad, B.D.; Narayana, K.L. Effect of MMT Clay on Mechanical, Thermal and Barrier Properties of Treated Aloevera Fiber/ PLA-Hybrid Biocomposites. *Silicon* **2020**, *12*, 1751–1760. [[CrossRef](#)]
24. Cao, M.; Cui, T.; Yue, Y.; Li, C.; Guo, X.; Jia, X.; Wang, B. Preparation and Characterization for the Thermal Stability and Mechanical Property of PLA and PLA/CF Samples Built by FFF Approach. *Materials* **2023**, *16*, 5023. [[CrossRef](#)] [[PubMed](#)]
25. Wang, Q.; Zhang, Q.; Kang, Y.; Wang, Y.; Liu, J. An investigation of preparation of continuous carbon fiber reinforced PLA prepreg filament. *Compos. Commun.* **2023**, *39*, 101530. [[CrossRef](#)]
26. Li, H.; Liu, B.; Ge, L.; Chen, Y.; Zheng, H.; Fang, D. Mechanical performances of continuous carbon fiber reinforced PLA composites printed in vacuum. *Compos. Part B Eng.* **2021**, *225*, 109277. [[CrossRef](#)]
27. Naranjo-Lozada, J.; Ahuett-Garza, H.; Orta-Castañón, P.; Verbeeten, W.M.; Sáiz-González, D. Tensile properties and failure behavior of chopped and continuous carbon fiber composites produced by additive manufacturing. *Addit. Manuf.* **2019**, *26*, 227–241. [[CrossRef](#)]
28. Yadav, P.; Sahai, A.; Sharma, R.S. Flexural Strength and Surface Profiling of Carbon-Based PLA Parts by Additive Manufacturing. *J. Inst. Eng. India Ser. C* **2021**, *102*, 1–11. [[CrossRef](#)]
29. Kumar Patro, P.; Kandregula, S.; Suhail Khan, M.; Das, S. Investigation of mechanical properties of 3D printed sandwich structures using PLA and ABS. *Mater. Proc.* **2023**. [[CrossRef](#)]
30. Zwawi, M. Structure Integrity and Fracture Prediction of PLA 3D-Printed Eye Grab Hooks with Different Cross Sections. *Procedia Struct. Integr.* **2022**, *37*, 1057–1064. [[CrossRef](#)]
31. Wu, W.Z.; Ye, W.L.; Wu, Z.C.; Geng, P.; Wang, Y.L.; Zhao, J. Influence of Layer Thickness, Raster Angle, Deformation Temperature and Recovery Temperature on the Shape-Memory Effect of 3D-Printed Poly(lactic Acid) Samples. *Materials* **2017**, *10*, 970. [[CrossRef](#)]
32. Sajjadi, S.A.; Ghasemi, F.A.; Rajaei, P.; Fasihi, M. Evaluation of fracture properties of 3D printed high impact polystyrene according to essential work of fracture: Effect of raster angle. *Addit. Manuf.* **2022**, *59*, 103191. [[CrossRef](#)]
33. Ayatollahi, M.R.; Nabavi-Kivi, A.; Bahrami, B.; Yahya, M.Y.; Khosravani, M.R. The influence of in-plane raster angle on tensile and fracture strengths of 3D-printed PLA specimens. *Eng. Fract. Mech.* **2020**, *237*, 107225. [[CrossRef](#)]
34. Nabavi-Kivi, A.; Ayatollahi, M.R.; Razavi, N. Investigating the effect of raster orientation on fracture behavior of 3D-printed ABS specimens under tension-tear loading. *Eur. J. Mech. A/Solids* **2023**, *99*, 104944. [[CrossRef](#)]
35. Gonabadi, H.; Chen, Y.; Yadav, A.; Bull, S. Investigation of the effect of raster angle, build orientation, and infill density on the elastic response of 3D printed parts using finite element microstructural modeling and homogenization techniques. *Int. J. Adv. Manuf. Technol.* **2022**, *118*, 1485–1510. [[CrossRef](#)]
36. Karimi, H.R.; Khedri, E.; Nazemzadeh, N.; Mohamadi, R. Effect of layer angle and ambient temperature on the mechanical and fracture characteristics of unidirectional 3D printed PLA material. *Mater. Today Commun.* **2023**, *35*, 106174. [[CrossRef](#)]
37. Anderson, T.L.; Anderson, T.L. *Fracture Mechanics: Fundamentals and Applications*; CRC Press: Boca Raton, FL, USA, 2005.
38. Sih, G.C.; Paris, P.C.; Irwin, G.R. On cracks in rectilinearly anisotropic bodies. *Int. J. Fract.* **1965**, *1*, 189–203. [[CrossRef](#)]
39. Rice, J.R. A Path Independent Integral and the Approximate Analysis of Strain Concentration by Notches and Cracks. *J. Appl. Mech.* **1968**, *35*, 379–386. [[CrossRef](#)]
40. Ning, F.; Cong, W.; Qiu, J.; Wei, J.; Wang, S. Additive manufacturing of carbon fiber reinforced thermoplastic composites using fused deposition modeling. *Compos. Part B Eng.* **2015**, *80*, 369–378. [[CrossRef](#)]
41. Hu, C.; Hau, W.N.J.; Chen, W.; Qin, Q.-H. The fabrication of long carbon fiber reinforced poly(lactic acid) composites via fused deposition modelling: Experimental analysis and machine learning. *J. Compos. Mater.* **2020**, *55*, 1459–1472. [[CrossRef](#)]
42. Arrigo, R.; Bartoli, M.; Malucelli, G. Poly(lactic Acid)-Biochar Biocomposites: Effect of Processing and Filler Content on Rheological, Thermal, and Mechanical Properties. *Polymers* **2020**, *12*, 892. [[CrossRef](#)]
43. Abdulla, F.A.; Hamid, K.L.; Ogaili, A.A.F.; Abdulrazzaq, M.A. Experimental study of Wear Rate Behavior for Composite Materials under Hygrothermal Effect. *IOP Conf. Ser. Mater. Sci. Eng.* **2020**, *928*, 022009. [[CrossRef](#)]
44. Ogaili, A.A.F.; Al-Ameen, E.S.; Kadhim, M.S.; Mustafa, M.N. Evaluation of mechanical and electrical properties of GFRP composite strengthened with hybrid nanomaterial fillers. *AIMS Mater. Sci.* **2020**, *7*, 93–102. [[CrossRef](#)]
45. Ogaili, A.A.F.; Abdulla, F.A.; Al-Sabbagh, M.N.M.; Waheeb, R.R. Prediction of Mechanical, Thermal and Electrical Properties of Wool/Glass Fiber based Hybrid Composites. In *IOP Conference Series: Materials Science and Engineering*; IOP Publishing: Bristol, UK, 2020; p. 022004.
46. Ogaili, A.A.F.; Jaber, A.A.; Hamzah, M.N. A methodological approach for detecting multiple faults in wind turbine blades based on vibration signals and machine learning. *Curved Layer. Struct.* **2023**, *10*, 20220214. [[CrossRef](#)]
47. Al-Ameen, E.S.; Abdulhameed, J.J.; Abdulla, F.A.; Ogaili, A.A.F.; Al-Sabbagh, M.N.M. Strength characteristics of pol-yester filled with recycled GFRP waste. *J. Mech. Eng. Res. Dev.* **2020**, *43*, 178–185.
48. Al-Ameen, E.S.; Al-Sabbagh, M.N.M.; Ogaili, A.A.F.; Kurji, A. Role of pre-stressing on anti-penetration properties for Kevlar/Epoxy composite plates. *Int. J. Nanoelectron. Mater.* **2022**, *15*, 293–302.
49. Al-Ameen, E.S.; Abdulla, F.A.; Ogaili, A.A.F. Effect of Nano TiO₂ on Static Fracture Toughness of Fiberglass/Epoxy Composite Materials in Hot Climate regions. *IOP Conf. Ser. Mater. Sci. Eng.* **2020**, *870*, 012170. [[CrossRef](#)]

50. Mohammed, S.A.; Al-Haddad, L.A.; Alawee, W.H.; Dhahad, H.A.; Jaber, A.A.; Al-Haddad, S.A. Forecasting the productivity of a solar distiller enhanced with an inclined absorber plate using stochastic gradient descent in artificial neural networks. *Multiscale Multidiscip. Model. Exp. Des.* **2023**, *7*, 1–11. [[CrossRef](#)]
51. Akasheh, F.; Aglan, H. Fracture toughness enhancement of carbon fiber-reinforced polymer composites utilizing additive manufacturing fabrication. *J. Elastomers Plast.* **2018**, *51*, 698–711. [[CrossRef](#)]
52. Oviedo, A.; Puente, A.; Bernal, C.; Pérez, E. Mechanical evaluation of polymeric filaments and their corresponding 3D printed samples. *Polym. Test.* **2020**, *88*, 106561. [[CrossRef](#)]
53. Jap, N.S.; Pearce, G.M.; Hellier, A.K.; Russell, N.; Parr, W.C.; Walsh, W.R. The effect of raster orientation on the static and fatigue properties of filament deposited ABS polymer. *Int. J. Fatigue* **2019**, *124*, 328–337. [[CrossRef](#)]
54. Khosravani, M.R.; Reinicke, T. Effects of printing parameters on the fracture toughness of 3D-printed polymer parts. *Procedia Struct. Integr.* **2023**, *47*, 454–459. [[CrossRef](#)]
55. Vălean, E.; Foti, P.; Berto, F.; Marşavina, L. Static and fatigue behavior of 3D printed smooth and notched PLA and short carbon fibers reinforced PLA. *Theor. Appl. Fract. Mech.* **2024**, *131*, 104417. [[CrossRef](#)]
56. Ogaili, A.A.F.; Hamzah, M.N.; Jaber, A.A. Integration of Machine Learning (ML) and Finite Element Analysis (FEA) for Predicting the Failure Modes of a Small Horizontal Composite Blade. *Int. J. Renew. Energy Res.* **2022**, *12*, 2168–2179. [[CrossRef](#)]
57. Ogaili, A.A.; Hamzah, M.N.; Jaber, A.A. Free Vibration Analysis of a Wind Turbine Blade Made of Composite Materials. In Proceedings of the International Middle Eastern Simulation and Modeling Conference, Baghdad, Iraq, 27–29 June 2022; pp. 27–29.

Disclaimer/Publisher’s Note: The statements, opinions and data contained in all publications are solely those of the individual author(s) and contributor(s) and not of MDPI and/or the editor(s). MDPI and/or the editor(s) disclaim responsibility for any injury to people or property resulting from any ideas, methods, instructions or products referred to in the content.